IEEE Journal of Translational Engineering in Health and Medicine

Received 17 July 2018; revised 27 October 2018; accepted 29 October 2018.
Date of publication 23 November 2018; date of current version 5 December 2019.

Digital Object Identifier 10.1109/JTEHM.2018.2880199

Intuitive Clinician Control Interface for a Powered Knee-Ankle Prosthesis: A Case Study

DAVID QUINTERO[1,2], (Student Member, IEEE), EMMA REZNICK[1], DANIEL J. LAMBERT[3], (Student Member, IEEE), SIAVASH REZAZADEH[1], (Member, IEEE), LESLIE GRAY[4], AND ROBERT D. GREGG[1,2], (Senior Member, IEEE)

[1]Department of Bioengineering, The University of Texas at Dallas, Richardson, TX 75080, USA
[2]Department of Mechanical Engineering, The University of Texas at Dallas, Richardson, TX 75080, USA
[3]Department of Electrical Engineering, The University of Texas at Dallas, Richardson, TX 75080, USA
[4]Department of Health Care Sciences, The University of Texas Southwestern Medical Center, Dallas, TX 75390, USA

CORRESPONDING AUTHOR: R. D. GREGG (rgregg@ieee.org)

This work was supported by the National Institute of Child Health and Human Development of the NIH under Awards DP2HD080349 and R01HD094772. The work of R. D. Gregg was supported by the Burroughs Wellcome Fund through the Career Award at the Scientific Interface.

ABSTRACT This paper presents a potential solution to the challenge of configuring powered knee-ankle prostheses in a clinical setting. Typically, powered prostheses use impedance-based control schemes that contain several independent controllers which correspond to consecutive periods along the gait cycle. This control strategy has numerous control parameters and switching rules that are generally tuned by researchers or technicians and not by a certified prosthetist. We propose an intuitive clinician control interface (CCI) in which clinicians tune a powered knee-ankle prosthesis based on a virtual constraint control scheme, which tracks desired periodic joint trajectories based on a continuous measurement of the phase (or progression) of gait. The interface derives virtual constraints from clinician-designed joint kinematic trajectories. An experiment was conducted in which a certified prosthetist used the control interface to configure a powered knee-ankle prosthesis for a transfemoral amputee subject during level-ground walking trials. While it usually takes engineers hours of tuning individual parameters by trial and error, the CCI allowed the clinician to tune the powered prosthesis controller in under 10 min. This allowed the clinician to improve several amputee gait outcome metrics, such as gait symmetry. These results suggest that the CCI can improve the clinical viability of emerging powered knee-ankle prostheses.

INDEX TERMS Prosthetics, robot control, legged locomotion, user interfaces.

I. INTRODUCTION

Persons living with limb loss above the knee generally use mechanically passive prostheses that dissipate energy instead of actively inputting energy to replicate normative biomechanics [1], [2]. Certified prosthetists have direct involvement in prescribing prostheses, manufacturing custom sockets, and fitting and tuning a prosthesis to improve an amputee patient's gait [3]–[5]. The mechanical damping resistance of the knee joint is often adjusted to control knee extension and flexion during gait to achieve better symmetry [6], while the ankle passively stores and releases energy in a carbon-fiber body.

Powered prostheses have motors that provide power at the joints to improve limb functionality [7]–[11]. There are several control strategies currently being developed for powered prostheses [12]. Generally, they consist of a heuristic rule-based control scheme, such as a finite state machine, that contains a different controller for each portion of the divided gait cycle [8]–[10], [13], [14]. These controllers typically emulate joint stiffness and damping (i.e., impedance), which tend to change across users and tasks. This presents a challenging tuning problem for powered knee-ankle prostheses, which have dozens of impedance parameters and switching rules that must be tuned by a technical expert (usually an engineer) who is very familiar with the effect of each parameter on the control system and the user's response. This technical process can take several hours for each user [15], [16], which is one of the major reasons that powered knee-ankle prostheses have not been commercialized for clinical use.

Recent work has attempted to unify discrete periods of the gait cycle under a single virtual constraint control strategy,

This work is licensed under a Creative Commons Attribution 3.0 License. For more information, see http://creativecommons.org/licenses/by/3.0/

which reduces the parameter space to a small set that generalizes well across amputee subjects [17], [18]. Originally proposed for the control of biped robots [19]–[22], virtual constraints are often defined as polynomial functions of a phase variable, which is a time-invariant, kinematic quantity that determines the progression during gait. Applied to powered prostheses, virtual constraint controllers provide user synchronization to changing walking speeds [18] and phase-shifting disturbances such as small slips/trips [23]. However, previous studies of this control method utilized fixed, normative joint trajectories, which do not provide the flexibility for clinicians to configure a powered prosthesis for a patient's individual needs.

Prosthetists have substantial influence on amputee patient outcomes [24], so it is important for them to be intimately involved in the tuning process of a powered prosthesis. Clinicians generally observe amputee joint kinematics as the patient ambulates with a prosthesis to determine the adjustments necessary to improve inter-limb symmetry and restore normative biomechanics. We propose an intuitive clinician control interface (CCI) as a tuning tool that leverages this clinical expertise to easily adjust the prosthetic joint kinematics, which are converted into virtual constraints using the methods of Quintero *et al.* [25] and Rezazadeh *et al.* [26] for control of the powered knee-ankle prosthesis. Our control framework is uniquely suited for this clinical interface based on its continuous representation of the joint kinematics [25]. The baseline joint trajectories are represented as Catmull-Rom splines [27] generated from normative able-bodied data [28], which the clinician can manipulate through control points that determine the joint angle and phase of kinematic landmarks within the gait cycle. The CCI tool is designed with several user-friendly manipulation and safety features to facilitate the configuration process.

This paper presents the design of the CCI tool in the context of the virtual constraint control system, which was used by a certified prosthetist to quickly and effectively tune a powered knee-ankle prosthesis for an amputee subject. This case study replicated a clinical session, where the prosthetist visually inspects the patient's gait and then manually tunes the device until the subject is comfortable and the clinician agrees that gait pathologies and inter-limb asymmetry have been minimized. The protocol was designed to be as close to what an amputee would encounter visiting his/her prosthetist regarding available equipment and time constraints. The experimental results show improvement in various gait pathology metrics based on the clinical intervention, indicating that the clinician's intention was realized. Furthermore, clinical tuning time was observed to be minimal, which helped avoid fatigue [29].

II. METHODS AND PROCEDURES

This section provides an overview of the CCI, how it represents joint trajectories for manipulation, user features for adjusting the trajectories, how the adjusted trajectories are implemented in the control system of a powered knee-ankle prosthesis, and the experimental protocol of the case study. The graphical user interface (GUI) of Fig. 1 was implemented using the GUIDE app development tool of MATLAB R2013b (Mathworks Inc., Natick, MA).

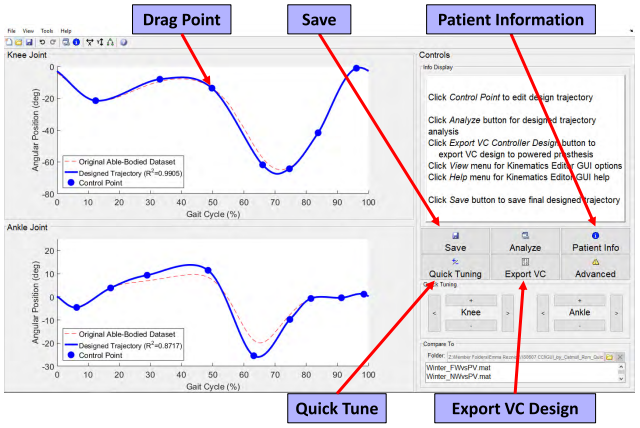

FIGURE 1. CCI GUI with commonly used features and visualizations of the knee (top) and ankle (bottom) angular position trajectories with respect to gait cycle percentage. Dragging the control points (blue dots) smoothly adjusts the joint trajectories. As an example, the ankle trajectory is modified (blue solid line) from the baseline trajectory (red dotted line) to have greater range of motion and an earlier push-off. The knee trajectory is minimally changed from the baseline and partly obscures the reference.

A. CCI INITIALIZATION

To begin the configuration process, the user must first open an existing patient file or create a new file. Creating a new file prompts the user to enter patient information such as subject ID, gender, age, and anatomical lower limb measurements. New files contain baseline knee and ankle kinematics (corresponding to a normal speed on level ground [28]), from which the clinician can tune the prosthesis for each patient. Opening an existing file displays the patient information and previously modified joint trajectories for that patient. All patient data is stored alongside the designed trajectories in a single MATLAB data file and can be referenced using the *Patient Info* button in Fig. 1. The help window guides the user step-by-step through common actions, as demonstrated in the supplemental video.

The next part describes how the joint trajectories are represented to facilitate their manipulation in the CCI.

B. CCI REPRESENTATION OF JOINT KINEMATICS

To provide manipulation points in Fig. 1, each joint's angular trajectory is represented by a set of N control points connected by $N-1$ piecewise Catmull-Rom splines [27]. This method interpolates between control points to create a set of piecewise cubic polynomials with matching tangent slopes at each control point. Hence, the velocity is continuous along this representation of the joint angle trajectory. Each control point p_i in the control points matrix,

$$C_P = [p_1, \cdots, p_N]^\top, \tag{1}$$

IEEE Journal of Translational Engineering in Health and Medicine

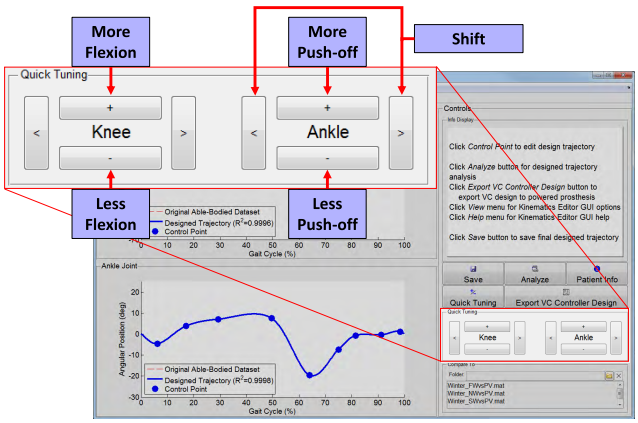

FIGURE 2. Quick tuning buttons allow for easily adjusting ankle push-off during stance and knee flexion during swing (key events of those joints). The plus (+) and minus (–) buttons increase and decrease the amplitude of the transition, and the left (<) and right (>) buttons move the transition earlier and later in the gait cycle, both respectively.

comprises an x and y coordinate indicating the temporal location (i.e., phase) in the gait cycle and the joint angular position, respectively. The points are listed in increasing order of the x coordinate. The beginning and end points in C_P are constrained to enforce periodicity of the trajectory.

For the baseline kinematics, an optimization routine fits a piecewise cardinal spline to able-bodied human joint kinematics for normal level-ground walking using data from [28]. This routine computes a limited number of control points that minimize the spline curve fitting error from the dataset. For each joint, the fitted spline is defined as the default (Baseline) joint trajectory that the clinician sees when starting a new patient profile. The clinician can then modify the prosthetic joint kinematics using the CCI features described below.

C. CCI FEATURES FOR CONFIGURING JOINT KINEMATICS

The CCI has the following features to assist the clinician in modifying the joint trajectories for patient-specific needs:

1) QUICK TUNING BUTTONS

The buttons highlighted in Fig. 2 allow the clinician to incrementally adjust the timing and amplitude of ankle push-off during terminal stance (45%-60%) and knee flexion during swing (50%-65%). These are the most commonly tuned features because ankle push-off is responsible for propelling the stride and swing knee flexion is responsible for toe clearance and the timing of knee extension in preparation for weight acceptance [30]. The associated control points are automatically modified to achieve the incremental changes. Left and right arrow buttons phase shift the curve along the gait cycle, and plus and minus buttons increase and decrease the angular amplitude along the y-axis. A clinician who desires a stronger ankle push-off earlier in the gait cycle, as in Fig. 1, may press the ankle plus (+) and left (<) buttons in the quick tuning panel to achieve this result.

2) DRAGGING CONTROL POINTS

Clicking and dragging any control point displays the modified curve in real-time for visual inspection. Having the capability to view the joint angular position and velocity plots, a novice user can gain insight into the full effect of the kinematic modifications. Moving a control point p_j to a new (x, y) location $\tilde{p}_j$ replaces the corresponding entry in the control points matrix subject to the monotonicity constraint $p_{j-1,1} < \tilde{p}_{j,1} < p_{j+1,1}$. For finer adjustments, control point coordinates can be specified through a manual numeric entry window as well.

A feature converts mouse drag operations into smooth adjustments across neighboring control points in real time. Part of the user-specified change $(\tilde{p}_j - p_j)$ is applied to the immediate surrounding control points p_{j-1} and p_{j+1} based on the relative spacing of $p_{j-2}, \ldots, p_{j+2}$, given by the scalar translation scaling coefficients

$$\gamma_1 = \frac{\|p_{j-1} - p_j\|}{\|p_{j-1} - p_{j-2}\| + \|p_{j-1} - p_j\|}, \tag{2}$$

$$\gamma_2 = \frac{\|p_{j+1} - p_j\|}{\|p_{j+1} - p_{j+2}\| + \|p_{j+1} - p_j\|}. \tag{3}$$

These apply the $\tilde{p}_j$ translation vector to the modified neighboring points

$$\tilde{p}_{j-1} = p_{j-1} + \gamma_1(\tilde{p}_j - p_j), \tag{4}$$

$$\tilde{p}_{j+1} = p_{j+1} + \gamma_2(\tilde{p}_j - p_j). \tag{5}$$

The piecewise splines are then re-optimized with the updated control points matrix containing $\tilde{p}_{j-1}, \tilde{p}_j, \tilde{p}_{j+1}$.

3) ADD/DELETE CONTROL POINTS

Under the *View* menu bar is the option to add/delete control points on the curve, giving the user more control over the placement of the piecewise polynomials. Inserting a new control point requires adding a new point p_j to the control points matrix, where $p_{j-1,1} < p_{j,1} < p_{j+1,1}$. Likewise, deleting a control point p_j removes it from the control points matrix.

4) SAFETY FEATURES

The safety features include limits on the joint angle range of motion, joint velocity, and sequential order of control points. For example, if a user attempts to increase push-off in a way that violates the velocity constraint, the CCI will highlight the offending section and alert the user that the modification exceeds the prosthesis safety limits (as demonstrated in the supplementary video). This allows the clinician to design joint kinematics that are feasible for the prosthetic leg to perform.

5) DISPLAY OF GAIT PERIODS

To further aid clinicians in using this interface, a feature displays gait period reference markers within commonly known periods of gait (e.g., Loading Response, Mid-stance, Pre-Swing, Mid-Swing, and Terminal Swing). When enabled,

the interface displays both the gait period name and highlighted region associated with the gait period hovered by the mouse.

6) COMPARISON TOOL

Additionally, the CCI lists previous amputee subject design files in a comparison toolbar for ease of comparing the current trajectory design to previous designs on the same figure. For instance, a clinician can review a subject's current design from a past clinical session to determine if additional kinematic changes are needed for the subject to improve their gait. Selecting a previous design file displays the position and velocity curves alongside the current design. This comparison feature can help clinicians track changes over time for individual subjects.

D. IMPLEMENTATION IN PROSTHETIC CONTROL SYSTEM

1) VIRTUAL CONSTRAINT DESIGN

Once the joint trajectories are finalized, the *Export VC Design* button (see Fig. 1) converts the clinician-designed trajectories into virtual constraint functions that are compiled into the real-time processor of the powered knee-ankle prosthesis for testing and evaluation.

The method of Discrete Fourier Transform (DFT) can be used to parameterize virtual constraints that represent the periodic joint kinematics of the human gait cycle [18]. The DFT first computes the frequency content of the clinician-designed trajectory for each joint. The frequency content is then used to reconstruct the desired trajectory as a function of an ideal, normalized phase variable $s \in [0, 1)$ as follows:

$$h^d(s) = \frac{1}{2}\alpha_0 + \frac{1}{2}\alpha_{\frac{L}{2}}\cos(\pi L s) + \sum_{w=1}^{W}\Big[\alpha_w \cos(\Omega_w s) - \beta_w \sin(\Omega_w s)\Big], \quad (6)$$

where $\Omega_w = 2\pi w$, W is the total number of frequency components, L is the number of samples in the trajectory, and α_w and β_w are the computed DFT coefficients.

The functional DFT representation above is used to define the virtual constraint output function for each joint:

$$y_i(q_i, s) = q_i - h_i^d(s), \quad (7)$$

where q_i is the measured angular position of joint i (with $i = k$ for the knee or $i = a$ for the ankle), and h_i^d is the desired angular position according to the phase variable s. The output function y_i represents tracking error from the desired kinematics and is thus driven towards zero by the following torque control law:

$$\tau_i = -K_{\mathrm{p}i} y_i - K_{\mathrm{d}i}\dot{q}_i, \quad (8)$$

where $K_{\mathrm{p}i} > 0$ is the proportional gain providing a virtual stiffness and $K_{\mathrm{d}i} > 0$ is the derivative gain for virtual damping at joint i. These control gains were manually tuned during a previous study with an able-bodied subject wearing a bypass adapter [31]. This Proportional-Derivative controller commands the joint torques to enforce the virtual constraints.

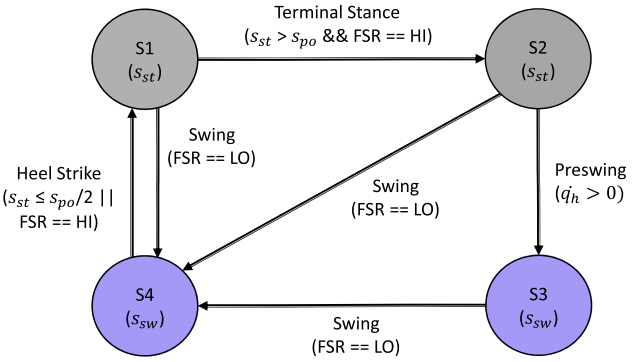

FIGURE 3. A finite state machine using a piecewise phase variable to perform forward walking. The gray circles refer to Eq. 9 and purple circles refer to Eq. 10. Between each state there are transition rules that evaluate s_{st} about ankle push-off threshold s_{po}, FSR sensing for ground foot contact (HI) or no contact (LO), or thigh velocity $\dot{q}_h$ changing sign during pre-swing.

2) PIECEWISE PHASE VARIABLE DESIGN

This study utilized the phase variable designed and tested in [26], which measures the thigh angle to determine the progression of the subject through the gait cycle. The velocity-independent nature of the selected phase variable naturally accommodates changes in speed, start and stop, and some volitional activities. The computation of the phase variable is done according to the finite state machine in Fig. 3. Depending on the state of the system, the phase variable s in (6) is determined from the stance equation or swing equation as follows:

$$s_{st}(q_h) = \frac{q_h^{max} - q_h}{q_h^{max} - q_h^{min}}\kappa, \quad (9)$$

$$s_{sw}(q_h) = 1 + \frac{1 - s_{st}^f}{q_h^{max} - q_h^{min,f}}(q_h - q_h^{max}), \quad (10)$$

where q_h is the global angle of the residual thigh (see Section III), q_h^{max} and q_h^{min} are the pre-set maximum and minimum thigh angle values (tunable for change of step length), and s_{st}^f and $q_h^{min,f}$ are the respective values of s_{st} and q_h at the moment of transition from state S2 to S3 or S4. Also, κ is a tunable parameter for the value of s_{st} at $q_h = q_h^{min}$, which thereby sets the stance to swing duration ratio. The variables s_{st}^f and $q_h^{min,f}$ adaptively change between strides to appropriately normalize s_{sw} and smooth the transition between the stance and swing phase variables. See [26] for further details on the controller design.

E. POWERED PROSTHESIS HARDWARE

The control system was implemented in a custom powered knee-ankle prosthesis for experiments with the CCI (Fig. 4). Both the knee and ankle contained a multi-stage transmission system to actuate their respective joint. The actuator consisted of a high speed Maxon EC-4pole 30, 200 Watt brushless direct current motor powered by a Elmo Gold Twitter R80/80 motor amplifier. The motor was connected to a

IEEE Journal of Translational Engineering in Health and Medicine

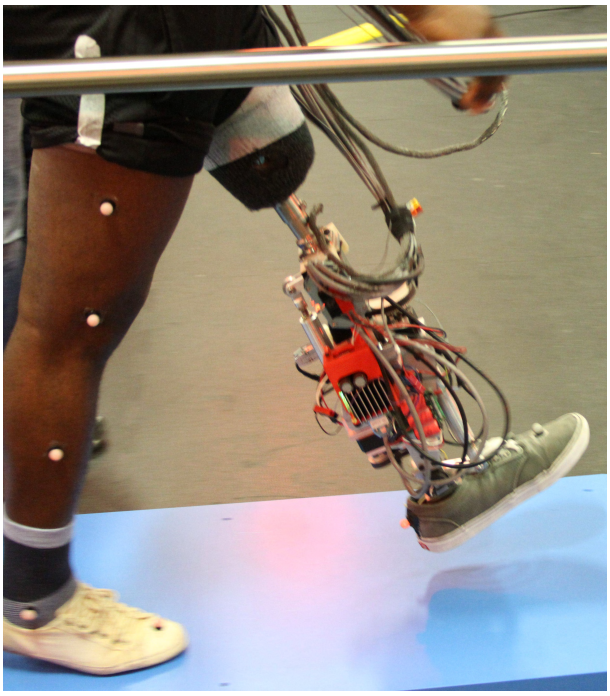

FIGURE 4. Photo of the transfemoral amputee subject wearing the powered knee-ankle prosthesis. Reflective markers were placed on the subject's lower body to collect kinematic data from a motion capture system during walking trials.

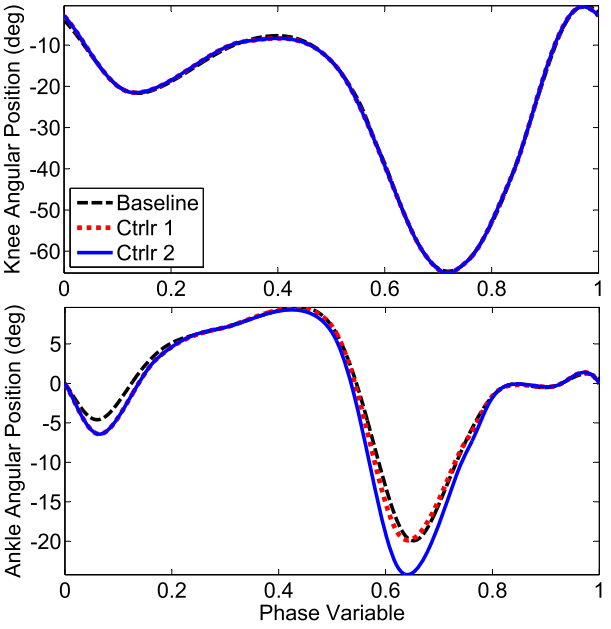

FIGURE 5. Clinician-designed knee (top) and ankle (bottom) trajectories versus baseline trajectories over the phase variable. Controller 1 (Ctrlr 1) had very minor adjustments to the knee, which were identical to Controller 2 (Ctrlr 2). Ankle push-off was increased in Controller 1 and even more in Controller 2. The latter controller also was given an earlier push-off. All these trajectories were exported from the CCI tool into the prosthesis virtual constraint controller for experimentation.

timing belt drive with sprockets giving a 4:1 reduction at the ankle and 2:1 at the knee. The sprockets were connected to a Nook 12-mm diameter, 2-mm lead ball screw connected to a lever arm that actuated the joints. The motor amplifiers were powered by an Agilent 6673A power supply.

A dSPACE DS1007 system with Freescale OorIQ P5020, 2 GHz processor was tethered to the prosthesis for control computation and data acquisition sampled at 1 kHz. A Tekscan FlexiForce A401 sensor was placed inside the pyramid adapter of the prosthetic foot to detect ground contact. US Digital EC35 encoder provided measurements of each joint angle. A LORD Microstrain 3DMGX4-25 inertial measurement unit was placed on top of the prosthetic knee joint to measure the global angle of the residual thigh for calculation of the phase variable. More detailed design specifications for the prosthesis can be found in [18] and [31].

F. EXPERIMENTAL SETUP & PROTOCOL

The experimental protocol was approved by the Institutional Review Boards of the University of Texas at Dallas and the University of Texas Southwestern Medical Center. Before the experiment took place, a clinical researcher was instructed how to use the interface over a period of about 15 minutes. This entailed manipulating the trajectories to affect the movement of the prosthesis and using the 'Quick Tuning' buttons and various other features. The clinical researcher was a practicing, certified, and licensed prosthetist for 14 years with no prior experience configuring a powered knee-ankle prosthesis.

The experimental setup included a ten-camera motion capture system (Vicon, Oxford, UK) utilizing Nexus Plug-in-Gait software to record kinematic parameters of a transfemoral amputee subject walking along a 5.3 m handrail walkway. The amputee subject had a height of 1.75 m, weight of 76.5 kg, left side amputation, and post-amputation time of 11 yrs. The subject had no prior experience using a powered prosthesis. Reflective markers were placed along key landmarks on the subject's body and prosthesis to capture 3D spatial coordinates, which fed into a 3D kinematic biped model to assess the kinematic changes effected by the clinician. The subject was asked to bring comfortable shorts that were adjusted so that no markers would be obscured from the motion capture cameras. The clinician attached and aligned the powered prosthesis to the subject's custom socket. Before recording data, the subject spent time acclimating to the powered prosthesis by walking overground with handrails. Acclimation was declared when the subject felt comfortable starting, stopping, and walking forward with the powered prosthesis.

The experiment entailed multiple passes (i.e., trials) of the subject walking the length of the handrails using the powered prosthesis. The subject was instructed to walk naturally without use of the handrails unless necessary to maintain balance, which was not required during data collection. The subject began with the default (Baseline) virtual constraints

designed from normal walking kinematics in [28]. Based on observations of the subject's gait, the clinical researcher used the CCI to iteratively tune the trajectories until the clinician and amputee subject agreed that the prosthesis was comfortable for daily walking and emulated normative biomechanics.

Because this case study was intended to emulate a clinical session, the number of trials was determined by the clinician during the experiment—based on when the clinician and subject were satisfied—rather than a priori to conduct statistical tests. Instead, clinical significance was investigated through summary statistics of outcome metrics such as spatial-temporal parameters and gait symmetry. For each controller, the strides of all trials ($n = 8$ to 11) were parsed into gait cycles to calculate these summary statistics.

III. RESULTS

A. CLINICIAN VIRTUAL CONSTRAINT DESIGN & OUTCOME

The clinician iteratively tuned the prosthesis with the amputee subject, creating two different clinically-tuned controllers. After observing the subject walking with the baseline controller, the clinician prescribed more ankle push-off. This involved using the CCI to increase ankle plantarflexion in the appropriate region of gait. Knee flexion was shifted slightly earlier during the swing period using the 'Quick Tuning' button. Once the desired trajectories were established, they were transformed into virtual constraints for the prosthesis controller by taking the DFT of the desired trajectories [18]. This is labeled as Controller 1. The amputee repeated forward walking trials with Controller 1 while the clinician observed.

After discussion, the subject provided feedback to the clinician requesting additional tuning at the ankle for more push-off. Additionally, the clinician observed that an adjustment in the timing of push-off was needed. These observations were implemented in Controller 2 for another iteration. The clinician and subject agreed that the knee motion occurred at the correct phase with appropriate magnitude, and consequently did not make additional adjustments. After the subject repeated forward walking trials with this new controller, the clinician performed a visual inspection and, with feedback from the subject, agreed that the second controller was tuned appropriately. Fig. 5 displays the baseline joint kinematics compared to the two clinical controllers. The clinician took a total of 10 minutes to tune the prosthesis.

Fig. 6 compares the prosthesis and residual limb measurements between walking trials of Baseline and Controller 2, where the subject started from rest at $t = 0$. Increased ankle push-off and knee flexion peaks were observed as speed increased for both Baseline and Controller 2, likely due to the subject putting more weight into the prosthesis to complete the ankle push-off [26]. The additional push-off designed into Controller 2 was realized in the prosthetic ankle trajectories, which had noticeably larger peaks than Baseline. The increased ankle push-off likely caused the faster progression of the phase variable in Controller 2 (i.e., faster forward speed). The increased ankle push-off also increased the thigh forward acceleration during swing (cf. [32]), which can explain the greater forward thigh range of motion for Controller 2, especially visible in the second stride.

B. SPATIAL-TEMPORAL PARAMETERS

Spatial-temporal parameters are often used to assess the performance of a human's locomotion [28], [33]. In this experiment, spatial-temporal parameters refer to step length (spatial), step time and swing time (temporal). Table 1 displays the mean and standard deviation of each parameter for both the prosthetic (P) and intact (I) legs across controllers. The clinician-tuned controllers encouraged convergence between the prosthetic leg parameters and intact leg parameters. These metrics show confidence of the subject with the prosthesis as well as improvements in gait symmetry, which is associated with functional mobility [34]. The difference in stance time between legs, a good indicator of uneven gaits, decreased by 15% with Controller 1 and 44% with Controller 2. The changes in stance and swing time affected the stance percentage (the percent of the gait cycle that the ipsilateral foot is on the ground) causing the percentage to converge closer to the accepted textbook value of 60% for normal walking [35].

C. GAIT PATHOLOGY RESULTS

Passive prosthesis users often develop compensatory strategies at their intact joints to propel the stride and promote toe clearance during swing. Powered knee-ankle prostheses can potentially mitigate these compensations by injecting energy during push-off while actively flexing the knee. Table 2 reports parameters associated with hip hiking, hip circumduction, and ankle vaulting. Vaulting is the compensation of early and excessive plantarflexion of the intact ankle during stance, which can be quantified by the peak value of the foot progression angle during mid-stance. Clinical tuning resulted in an overall decrease in ankle vaulting. This is likely due to the prescribed increase in ankle push-off, which propels the prosthesis into swing for greater toe clearance.

Hip hiking and circumduction are compensations involving excessive range of motion in pelvic obliquity and hip abduction in the frontal plane [36]. As reported in Table 2, Controller 1 exhibited an average decrease in hip abduction on both sides, along with a slight decrease in pelvic obliquity on the prosthetic side. Controller 2 also exhibited a decrease in hip abduction on the prosthetic side, but increases in pelvic range of motion on both sides.

The symmetry ratio (SR) of spatial-temporal parameters is often used to identify gait pathologies associated with asymmetries between legs. This ratio is defined as

$$SR = \frac{\Upsilon_{\text{prosthetic}}}{\Upsilon_{\text{intact}}}, \tag{11}$$

where Υ refers to the parameter being evaluated [37]. A perfectly symmetrical gait will have a value of one, whereas a ratio greater than one favors the prosthetic side. According to Table 2, the SR for step length improved with each iteration

IEEE Journal of Translational Engineering in Health and Medicine

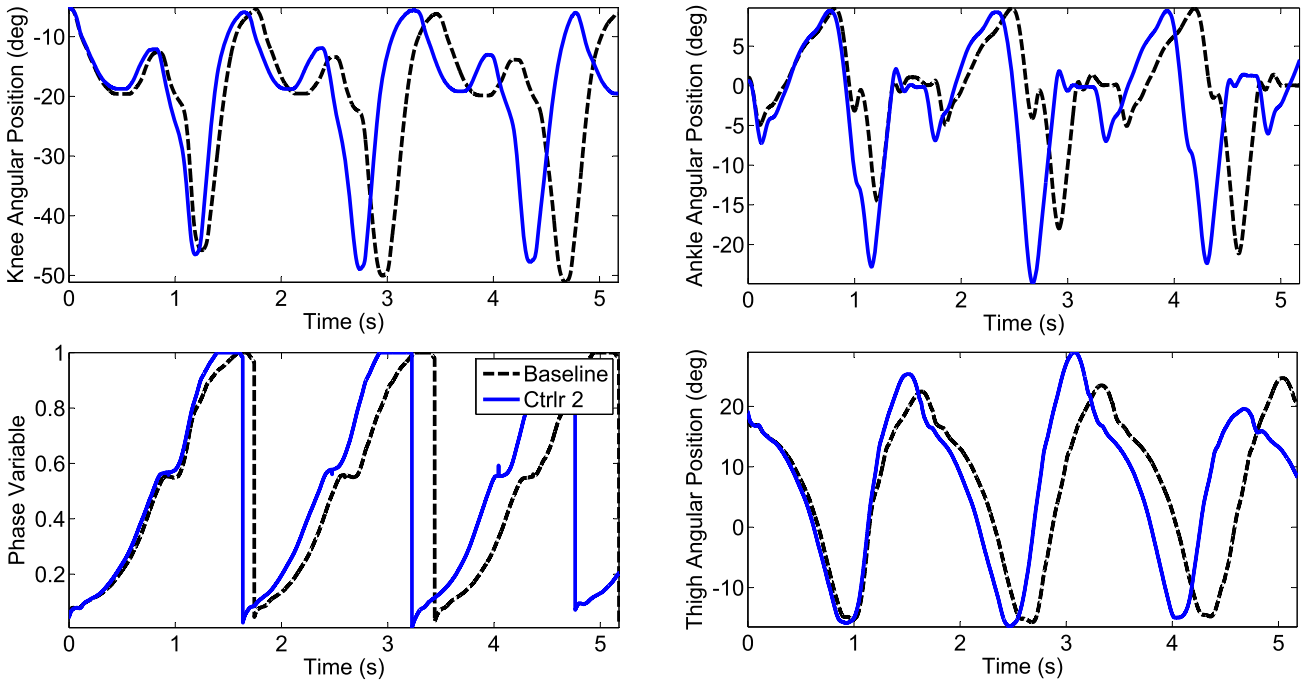

FIGURE 6. Measured signals of the prosthetic knee angle (top left), prosthetic ankle angle (top right), phase variable (bottom left), and residual thigh angle (bottom right) over consecutive strides for a forward walking trial of the Baseline controller versus Controller 2 (Ctrlr 2). The time sequences of the separate trials were aligned with respect to their first phase variable measurement. As the phase variable progressed from 0 to 1 (bottom left), the joint kinematics progressed through the designed trajectories (top). The knee trajectories were similar between controllers by design. Controller 2 had a noticeably larger ankle push-off than Baseline, resulting in faster phase variable progression and greater thigh range of motion.

TABLE 1. Mean(SD) of spatial-temporal parameters on prosthetic (P) and intact (I) sides.

	Stance Time [s]		Swing Time [s]		Step Length [m]		Stance Percentage [%]	
	P	I	P	I	P	I	P	I
Baseline	0.82 (0.08)	1.11 (0.06)	0.72 (0.01)	0.40 (0.00)	0.51 (0.01)	0.47 (0.01)	54.9 (1.69)	70.9 (1.64)
Controller 1	0.91 (0.12)	1.17 (0.11)	0.65 (0.06)	0.41 (0.02)	0.48 (0.03)	0.45 (0.10)	58.2 (4.87)	73.7 (2.64)
Controller 2	0.88 (0.05)	1.07 (0.19)	0.65 (0.07)	0.47 (0.06)	0.54 (0.04)	0.54 (0.03)	57.6 (3.48)	69.3 (3.41)

TABLE 2. Mean(SD) of measures of gait pathology on prosthetic (P) and intact (I) sides.

	Hip ROM [deg]		Pelvic ROM [deg]		Vaulting [deg]	Symmetry Ratios		
	P	I	P	I	I	Step Length	Stance Time	Swing Time
Baseline	7.09 (0.32)	10.61 (0.74)	7.68 (1.07)	3.35 (0.80)	14.50 (1.57)	0.93 (0.01)	1.33 (0.08)	0.65 (0.05)
Controller 1	5.44 (1.33)	9.06 (1.15)	6.58 (1.25)	3.77 (0.36)	13.61 (2.28)	0.94 (0.11)	1.28 (0.06)	0.64 (0.05)
Controller 2	6.35 (1.24)	12.27 (1.77)	8.14 (2.48)	5.18 (1.26)	14.03 (1.50)	1.02 (0.05)	1.23 (0.04)	0.74 (0.09)

of the clinical tuning process. Stance and swing time also exhibited a slight progression towards symmetry.

IV. DISCUSSION AND CONCLUSION

We developed an intuitive interface for clinicians to quickly configure a powered knee-ankle prosthesis for subject-specific needs. Instead of tuning dozens of impedance parameters and switching rules, our approach leverages clinical expertise to configure a continuous representation of the joint kinematics in a virtual constraint control scheme. To demonstrate feasibility, a certified prosthetist used the CCI to configure a powered knee-ankle prosthesis for a transfemoral amputee subject. Controllers 1 and 2 appeared to realize the prosthetist's desired kinematics, improving several aspects of the subject's gait.

The convergence of spatial-temporal parameters suggests the subject had more control [34] and more even loading between limbs, which could reduce pain and joint degeneration over time [38]. These improvements were primarily achieved by changing the timing and magnitude of push-off to restore healthy locomotor function and energetics with the powered prosthesis [39], [40]. These adjustments enabled the subject to spend more time on the prosthetic leg during stance and fully leverage push-off, resulting in prosthetic foot

clearance with less vaulting on the intact side. Hip hiking and circumduction did not exhibit consistent changes during the tuning process, which may be due to the weight of the robotic prosthetic leg. Moreover, these and other quantities have relatively high standard deviation because of the short walkway and limited number of trials during the emulated clinical session.

This limited case study motivates future studies in several directions. Having established feasibility of clinicians using the CCI system to affect powered knee-ankle prosthesis performance within the constraints of a clinical session, a more extensive outcomes study should be conducted with sufficient trials and subjects for statistical comparisons between take-home and powered prosthetic legs. Additional acclimation time may allow further reductions in compensations, which are learned over long-term use of a conventional prosthesis. Future studies would also benefit from newer powered prostheses with higher torque-to-weight ratios as in [41]. Finally, the CCI tool can be extended to configure the kinematics of additional tasks such as walking on stairs and inclines, and new features such as real-time feedback of spatial-temporal parameters could be added to further assist the clinician.

ACKNOWLEDGEMENT

The authors thank Christopher Nesler and Nikhil Divekar for their help during the experiments. They would also like to thank Kyle Embry for his editorial contributions and Mark Yeatman for his contributions to the GUI. The content is solely the responsibility of the authors and does not necessarily represent the official views of the NIH.

REFERENCES

[1] S. Kirker, S. Keymer, J. Talbot, and S. Lachmann, "An assessment of the intelligent knee prosthesis," *Clin. Rehabil.*, vol. 10, no. 3, pp. 267–273, Aug. 1996.

[2] J. L. Johansson, D. M. Sherrill, P. O. Riley, P. Bonato, and H. Herr, "A clinical comparison of variable-damping and mechanically passive prosthetic knee devices," *Amer. J. Phys. Med. Rehabil.*, vol. 84, no. 8, pp. 563–575, Aug. 2005.

[3] M. Zahedi, W. Spence, S. Solomonidis, and J. Paul, "Alignment of lower-limb prostheses," *J. Rehabil. Res. Develop.*, vol. 23, no. 2, pp. 2–19, Apr. 1986.

[4] B. Greitemann, "Prosthetics and orthotics: Prosthetic fitting in lower extremity in transfemoral amputation," *Zeitschrift Orthopädie Unfallchirurgie*, vol. 155, no. 6, pp. 737–749, Dec. 2017.

[5] R. Seymour, *Prosthetics and Orthotics: Lower Limb and Spinal*. Baltimore, MD, USA: Williams & Wilkins, Feb. 2002.

[6] J. Uchytil, D. Jandacka, D. Zahradnik, R. Farana, and M. Janura, "Temporal–spatial parameters of gait in transfemoral amputees: Comparison of bionic and mechanically passive knee joints," *Prosthetics Orthotics Int.*, vol. 38, no. 3, pp. 199–203, 2014.

[7] J. Hitt, T. Sugar, M. Holgate, R. Bellman, and K. Hollander, "Robotic transtibial prosthesis with biomechanical energy regeneration," *Ind. Robot*, vol. 36, no. 5, pp. 441–447, 2009.

[8] F. Sup, A. Bohara, and M. Goldfarb, "Design and control of a powered transfemoral prosthesis," *Int. J. Robot Res.*, vol. 27, no. 2, pp. 263–273, Feb. 2008.

[9] B. E. Lawson, J. Mitchell, D. Truex, A. Shultz, E. Ledoux, and M. Goldfarb, "A robotic leg prosthesis: Design, control, and implementation," *IEEE Robot. Autom. Mag.*, vol. 21, no. 4, pp. 70–81, Dec. 2014.

[10] E. J. Rouse, L. M. Mooney, and H. M. Herr, "Clutchable series-elastic actuator: Implications for prosthetic knee design," *Int. J. Robot. Res*, vol. 33, no. 13, pp. 1611–1625, Oct. 2014.

[11] D. S. Pieringer, M. Grimmer, M. F. Russold, and R. Riener, "Review of the actuators of active knee prostheses and their target design outputs for activities of daily living," in *Proc. IEEE Int. Conf. Rehab. Robot.*, Jul. 2017, pp. 1246–1253.

[12] M. R. Tucker *et al.*, "Control strategies for active lower extremity prosthetics and orthotics: A review," *J. Neuroeng. Rehabil.*, vol. 12, p. 1, Jan. 2015.

[13] S. K. Au and H. M. Herr, "Powered ankle-foot prosthesis," *IEEE Robot. Autom. Mag.*, vol. 15, no. 3, pp. 52–59, Sep. 2008.

[14] F. Sup, H. A. Varol, and M. Goldfarb, "Upslope walking with a powered knee and ankle prosthesis: Initial results with an amputee subject," *IEEE Trans. Neural Syst. Rehabil. Eng.*, vol. 19, no. 1, pp. 71–78, Feb. 2011.

[15] A. M. Simon *et al.*, "Configuring a powered knee and ankle prosthesis for transfemoral amputees within five specific ambulation modes," *PLoS ONE*, vol. 9, no. 6, p. e99387, Jun. 2014.

[16] A. H. Shultz, B. E. Lawson, and M. Goldfarb, "Running with a powered knee and ankle prosthesis," *IEEE Trans. Neural Syst. Rehabil. Eng.*, vol. 23, no. 3, pp. 403–412, May 2015.

[17] R. D. Gregg, T. Lenzi, L. J. Hargrove, and J. W. Sensinger, "Virtual constraint control of a powered prosthetic leg: From simulation to experiments with transfemoral amputees," *IEEE Trans. Robot.*, vol. 30, no. 6, pp. 1455–1471, Dec. 2014.

[18] D. Quintero, D. J. Villarreal, D. J. Lambert, S. Kapp, and R. D. Gregg, "Continuous-phase control of a powered knee–ankle prosthesis: Amputee experiments across speeds and inclines," *IEEE Trans. Robot.*, vol. 34, no. 3, pp. 686–701, Jun. 2018.

[19] E. R. Westervelt, J. W. Grizzle, C. Chevallereau, J. H. Choi, and B. Morris, *Feedback Control of Dynamic Bipedal Robot Locomotion*. Boca Raton, FL, USA: CRC Press, 2007.

[20] A. Ramezani, J. W. Hurst, K. A. Hamed, and J. W. Grizzle, "Performance analysis and feedback control of ATRIAS, a three-dimensional bipedal robot," *ASME J. Dyn. Syst., Meas., Control*, vol. 136, no. 2, p. 021012, Dec. 2013.

[21] K. Sreenath, H.-W. Park, I. Poulakakis, and J. W. Grizzle, "A compliant hybrid zero dynamics controller for stable, efficient and fast bipedal walking on MABEL," *Int. J. Robot. Res.*, vol. 30, no. 9, pp. 1170–1193, Sep. 2010.

[22] A. E. Martin, D. C. Post, and J. P. Schmiedeler, "Design and experimental implementation of a hybrid zero dynamics-based controller for planar bipeds with curved feet," *Int. J. Robot. Res.*, vol. 33, no. 7, pp. 988–1005, May 2014.

[23] D. J. Villarreal, H. A. Poonawala, and R. D. Gregg, "A robust parameterization of human gait patterns across phase-shifting perturbations," *IEEE Trans. Neural Syst. Rehabil. Eng.*, vol. 25, no. 3, pp. 265–278, Mar. 2017.

[24] I. Gaunaurd *et al.*, "Use of and confidence in administering outcome measures among clinical prosthetists: Results from a national survey and mixed-methods training program," *Prosthetics Orthotics Int.*, vol. 39, no. 4, pp. 314–321, Aug. 2015.

[25] D. Quintero, A. E. Martin, and R. D. Gregg, "Toward unified control of a powered prosthetic leg: A simulation study," *IEEE Trans. Control Syst. Technol.*, vol. 26, no. 1, pp. 305–312, Jan. 2018.

[26] S. Rezazadeh, D. Quintero, N. Divekar, and R. D. Gregg, "A phase variable approach to volitional control of powered knee-ankle prostheses," in *Proc. IEEE/RSJ Int. Conf. Intell. Robots Syst.*, Oct. 2018, pp. 1–7.

[27] E. Catmull and R. Rom, "A class of local interpolating splines," in *Computer Aided Geometric Design*. Amsterdam, The Netherlands: Elsevier, Dec. 1974, pp. 317–326.

[28] D. A. Winter, *Biomechanics and Motor Control of Human Movement*. Hoboken, NJ, USA: Wiley, Oct. 2009.

[29] G. K. Klute, J. S. Berge, M. S. Orendurff, R. M. Williams, and J. M. Czerniecki, "Prosthetic intervention effects on activity of lower-extremity amputees," *Arch. Phys. Med. Rehabil.*, vol. 87, no. 5, pp. 717–722, May 2006.

[30] J. H. Bowker and J. W. Michael, Eds., *Atlas of Limb Prosthetics: Surgical, Prosthetic, and Rehabilitation Principles*, 2nd ed. Rosemont, IL, USA: American Academy of Orthopaedic Surgeons, 2002.

[31] D. Quintero, D. J. Villarreal, and R. D. Gregg, "Preliminary experiments with a unified controller for a powered knee-ankle prosthetic leg across walking speeds," in *Proc. IEEE/RSJ Int. Conf. Intell. Robots Syst.*, Oct. 2016, pp. 5427–5433.

[32] S. Lipfert, M. Günther, D. Renjewski, and A. Seyfarth, "Impulsive ankle push-off powers leg swing in human walking," *J. Exp. Biol.*, vol. 217, no. 8, pp. 1218–1228, Apr. 2014.

[33] J. Perry and J. Burnfield, *Gait Analysis: Normal and Pathological Function*. Thorofare, NJ, USA: Slack-Incorporated, Jun. 2010.

[34] K. K. Patterson, W. H. Gage, D. Brooks, S. E. Black, and W. E. McIlroy, "Evaluation of gait symmetry after stroke: A comparison of current methods and recommendations for standardization," *Gait Posture*, vol. 31, no. 2, pp. 241–246, Feb. 2010.

[35] J. Perry and J. M. Burnfield, "Gait analysis: Normal and pathological function," *J. Sports Sci. Med.*, vol. 9, no. 2, p. 353, Jun. 2010.

[36] A. Armannsdottir, R. Tranberg, G. Halldorsdottir, and K. Briem, "Frontal plane pelvis and hip kinematics of transfemoral amputee gait. Effect of a prosthetic foot with active ankle dorsiflexion and individualized training—A case study," *Disab. Rehabil., Assistive Technol.*, vol. 13, no. 4, pp. 1–6, Oct. 2017.

[37] H. Sadeghi, P. Allard, F. Prince, and H. Labelle, "Symmetry and limb dominance in able-bodied gait: A review," *Gait Posture*, vol. 12, no. 1, pp. 34–45, Sep. 2000.

[38] L. Nolan, A. Wit, K. Dudziñski, A. Lees, M. Lake, and M. Wychowañski, "Adjustments in gait symmetry with walking speed in trans-femoral and trans-tibial amputees," *Gait Posture*, vol. 17, no. 2, pp. 142–151, Apr. 2003.

[39] P. H. Tzu-Wei, K. A. Shorter, P. G. Adamczyk, and A. D. Kuo, "Mechanical and energetic consequences of reduced ankle plantarflexion in human walking," *J. Exp. Biol.*, vol. 218, no. 22, pp. 3541–3550, Nov. 2015.

[40] K. E. Zelik and P. G. Adamczyk, "A unified perspective on ankle push-off in human walking," *J. Exp. Biol.*, vol. 219, no. 23, pp. 3676–3683, Nov. 2016.

[41] T. Elery, S. Rezazadeh, C. Nesler, J. Doan, H. Zhu, and R. Gregg, "Design and benchtop validation of a powered knee-ankle prosthesis with high-torque, low-impedance actuators," in *Proc. IEEE Int. Conf. Robot. Autom.*, May 2018, pp. 2788–2795.